Jordan Journal of Civil Engineering, Volume **16**, No. **4, 2022**

Influence of Crest Roughness on Weir Flow Conditions for Improving Nappe Stability

M. A. Khodier [1)*] ***and B. P. Tullis*** [2)]

[1)] Dept. of Civil Engineering, Yarmouk University, P. O. Box 566, Irbid, Jordan.
E-Mail: mohanad.khodier@yu.edu.jo * Corresponding Author.
[2)] Utah Water Research Laboratory, Dept. of Civil and Environmental Engineering, Utah State Univ., 8200 Old Main Hill, Logan, UT 84322-8200. E-Mail: blake.tullis@usu.edu

ABSTRACT

Low head nappe flow over hydraulic structures (such as weirs and fountains) can generate significant noise and pressure waves, through nappe oscillation creating the potential for a negative impact on the hydraulic structure safety and the surrounding environment. One potentially effective mitigation technique involves increasing the physical roughness of the weir crest surface. The exact phenomena (e.g. increased local turbulence, disrupted boundary layer growth, roughened air-water interface, … etc.) generated by the roughened crest surface responsible for mitigating the development of nappe oscillation isn't clear. In an effort to better understand the influence of weir crest surface roughness on nappe instabilities, an experimental investigation was conducted using a laboratory-scale linear weir with three different crest shapes (rectangular, quarter-round and half-round) to investigate changes in nappe-velocity profiles relative to smooth and artificially roughened weir crests. Artificially roughening a weir crest affected nappe-velocity profiles, discharge coefficients and nappe trajectory profiles, relative to the smooth crest conditions. Maximum horizontal velocities decrease with increasing crest roughness, particularly for smaller unit discharges. Roughening the weir crest improved nappe stability; however, adding crest roughness also reduced the hydraulic efficiency of the weir as noted by a reduction in discharge coefficient.

KEYWORDS: Nappe, Oscillation, Particle Image Velocimetry (PIV), Roughness, Unaerated.

INTRODUCTION

Weirs represent one of the more commonly used hydraulic structures in water conveyance systems, often used for flow diversion, flow measurement and reservoir outlet flow control, among others. The falling sheet of water downstream of the weir, referred to as the nappe, can under certain conditions exhibit an oscillating behavior that can generate significant noise and potentially cause damage to the hydraulic structures (Petrikat, 1958; Simmons, 1964; Chanson, 2002). Nappe behavior and instability have been studied experimentally and analytically by numerous researchers (Squire, 1953; Taylor, 1959; Schwartz, 1966; Barlow et al., 2010; Anderson, 2014; Khodier and Tullis, 2017).

Some studies have focused on the remediation of the nappe oscillation. Water et al. (1980) conducted an investigation of the spillway discharge noise at Avon dam. Utilizing physical models of varied size scales, different techniques were identified for suppressing nappe oscillation. Some effective mitigation techniques included adding a radius or bullnose on the downstream edge of the crest, adding angle iron on the upstream edge of the crest, adding splitters or roughening to the quarter-round crest. Schwartz (1966) also reported that nappe oscillations could be eliminated by roughening the crest boundary. Schwartz speculated that the instability of the boundary layer on the weir crest might play a significant role in determining the frequency of oscillation. Lodomez et al. (2019) studied the effectiveness of various crest modifications to reduce the nappe oscillation. They tested three mitigation solutions: 12

Received on 27/3/2022.
Accepted for Publication on 11/8/2022.

configurations with projecting elements, 5 configurations with deflectors and 1 configuration with a step. In general, all three mitigations were effective in reducing the nappe oscillation while limiting the reduction in discharge efficiency by less than 3%. Anderson and Tullis (2014) also verified the effectiveness of crest roughening to mitigate nappe oscillations.

A few studies have focused on the influences of artificially roughened weir crests on flow conditions, excluding nappe instability. Othman et al. (2011) reported that discharge coefficients for cylindrical crested weirs decreased with increasing surface roughness for all tested flow-rate conditions. Similarly, Jalil et al. (2014) and Parilkova et al. (2012) reported a decrease in discharge-coefficient values for broad crested weirs with increasing surface roughness. Decreasing discharge coefficients is an indication of decreased hydraulic efficiency.

Felder and Islam (2016) evaluated flow patterns, water surface profiles and pressure distributions over an artificially roughened large-crest embankment weir. The roughened crest caused the location of maximum velocity to move higher up in the water column (farther away from the crest), relative to a smooth-crest velocity profile. Also, the dimensionless pressure distributions showed some deviation from hydrostatic pressure for both smooth crest and rough crest, suggesting more dependence on the crest longitudinal profile (radius of curvature, … etc.) than boundary roughness. They also reported a reduction in embankment weir discharge with increasing surface roughness. Ghobadian et al. (2013) studied the effects of roughness on flow hydraulics over a circular weir at different flow conditions. They concluded that the upstream water level over the weir increases as the weir surface roughness increases. Also, they observed that the velocity profile over the weir becomes more uniform with a higher average velocity as the weir surface roughness increases. A recent numerical study by Qian et al. (2021) was performed to better understand the effect of weir roughness on the discharge performance under free and submerged conditions. They concluded that the effect of weir roughness on the discharge is significant for higher roughness height. Hayder (2017) studied experimentally the influence of adding semicircular rough elements on the flow conditions for the bed hydraulic jump stilling basin. He observed that adding a rough element to the bed hydraulic jump stilling basin increases the shear force and reduces the upstream and downstream depths of the flow.

Adding roughness to a weir crest likely results in various localized flow field responses (e.g. increased turbulence, disruption of the boundary layer development, a roughened air-water interface downstream of the weir, … etc.); however, the specific phenomena associated with weir crest roughening responsible for mitigating nappe oscillation are still unclear.

In an effort to better understand the flow-field response to crest roughening and the potential impact on improved nappe stability, an experimental investigation was conducted to evaluate flow-field response to rough and smooth weir crests of varying shape; specifically: rectangular crest (REC), quarter-round crest (QRC) and half-round crest (HRC). The associated streamwise velocity flow-field responses were documented using a non-intrusive Particle Image Velocimetry (PIV) velocity measurement system over a range of unit discharges.

Experimental Setup

All experiments were carried out at the Utah Water Research Laboratory (UWRL) at Utah State University. Weir flow experiments were conducted in a 9m long, 1.83m wide and 1.22m deep flume (see Figure 1-a), with the weir perpendicular to the channel centerline and extending the full width of the channel (i.e., suppressed weir). Water from a nearby reservoir was supplied to the flume *via* a 0.50 m diameter pipe. Flow straighteners (honeycomb) and a floating wave suppressor were placed 0.40 m downstream from the supply pipe outlet to reduce turbulence and improve approach flow uniformity. Flow rates were measured using a calibrated Venturi flow meter (±0.25% accuracy) and the upstream flow depth was measured using a precision point gauge installed 5 m upstream from the weir.

The small prototype-scale laboratory weir was 1.83 m long (L), 1.10 m tall (P), with a thickness of 0.076 m in the direction of flow. Three removable/interchangeable crest sections (REC, QRC and HRC) were fabricated from high-density polyethylene sheeting material (see Figure 1-b). The crests were roughened by overlaying different hardware cloth materials (see Figure 1-c). Roughness material 1 (R_1) was a square wire mesh (10.5

mm square) with a wire thickness of 2.6 mm. Roughness material 2 (R_2) was an expanded metal lathe with a thickness of 4.3 mm. These roughness materials were selected, because they represented non-permanent materials that could be added to existing weir structures to improve nappe stability. Unlike granular materials (e.g. sandpaper, … etc.) that have been used to roughen crests, a singular geometric parameter (e.g. average grain size) does not adequately describe the hardware cloth materials used herein. Consequently, material thicknesses and photographs are provided for material descriptive purposes. Due to the highly porous nature of R_1 and R_2 (see Figure 3-c), the smooth (non-roughened) weir crest elevation was maintained as the reference elevation for the roughened crest conditions, with R_1 and R_2 considered as crest roughness overlays rather than augmentations to the crest profile. A non-vented nappe condition was maintained for all tests (i.e., natural aeration of the cavity behind the nappe occurred, but was not vented to the atmosphere through a vent pipe or similar, see Figure 1-a). To support weir-flow visualization and velocity-field documentation via the PIV instrument, a section of flume wall adjacent to the weir was made of clear acrylic. The flow was seeded with nearly neutrally buoyant hollow micro-spherical glass particles with a diameter of 10 μm and a density of 1.10±0.05 g/cc. As part of the PIV data collection system, the flow field was illuminated with a frequency-doubled pulsed Nd:YAG (neodymium-doped yttrium-aluminum-garnet) laser light sheet with a wavelength of 532 μm, oriented parallel to the flow direction (see Figure 1-a). The scattered light from the first exposure and the second exposure of the seeded particles was recorded in double-frame images by a CCD camera (1376×1040 pixels resolution) operating at 15 Hz.

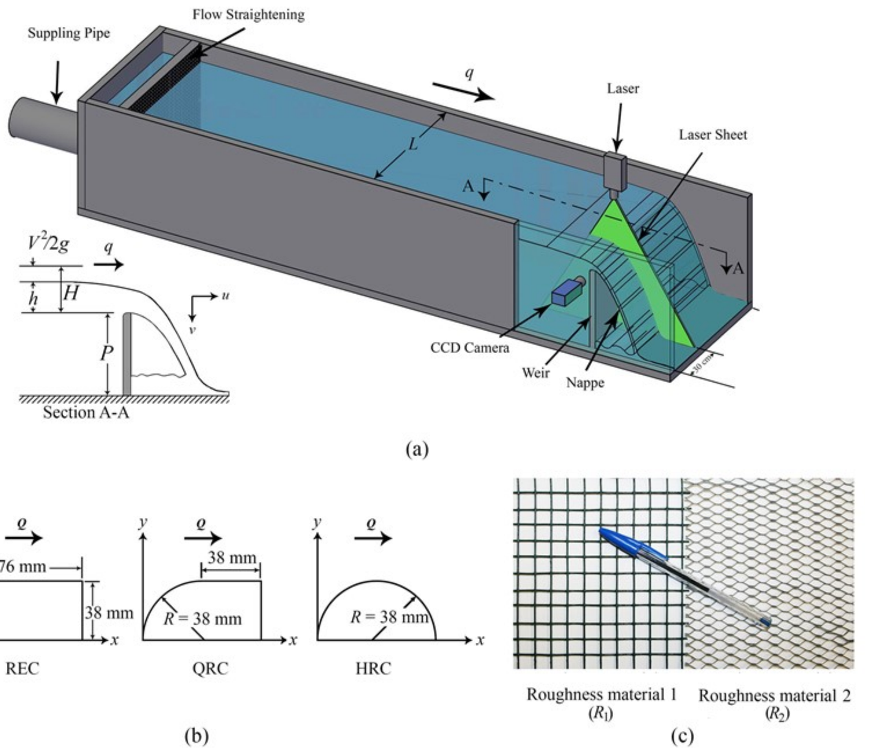

Figure (1): (a) Schematic of flume facilities and PIV set-up, (b) Weir-crest shapes and (c) Metal mesh used as roughness

For the smooth crest, velocity data was collected for unit discharges ranging from 4×10^{-3} to 36×10^{-3} m^2/s with an increment of 4×10^{-3} m^2/s (i.e., nine different discharges). For the roughened crest configurations, velocity data was collected for unit discharges of 4×10^{-3}, 8×10^{-3}, 16×10^{-3} and 32×10^{-3} m^2/s. From the smooth-crest tests, it was observed that the QRC and REC crest profiles developed self-induced nappe oscillations at the low and high discharges (i.e., the midrange discharge did not). It was found that adding the roughness materials (R_1 and R_2) to the crest surface suppressed the oscillation for all unit discharges and crest shapes evaluated. Adding a similar hardware cloth with a material thickness < 2.0 mm was ineffective in mitigating nappe oscillation. Consequently, the R_1 and R_2 materials were used in this investigation.

The discharge coefficient (C_d), as defined in one version of the standard weir equation [Eq. (1)], is an important dimensionless hydraulic weir parameter. Higher C_d values mean higher hydraulically weir efficiency (i.e., producing a higher discharge for a common upstream head).

$$Q = \frac{2}{3} C_d L \sqrt{2g} H^{3/2} \quad (1)$$

In Eq. (1), Q is the weir discharge, g is the gravitational acceleration constant and H is the total upstream head ($V^2/2g + h$, where V is the upstream cross-sectional average velocity and h is the upstream flow depth measured relative to the "smooth" weir crest elevation).

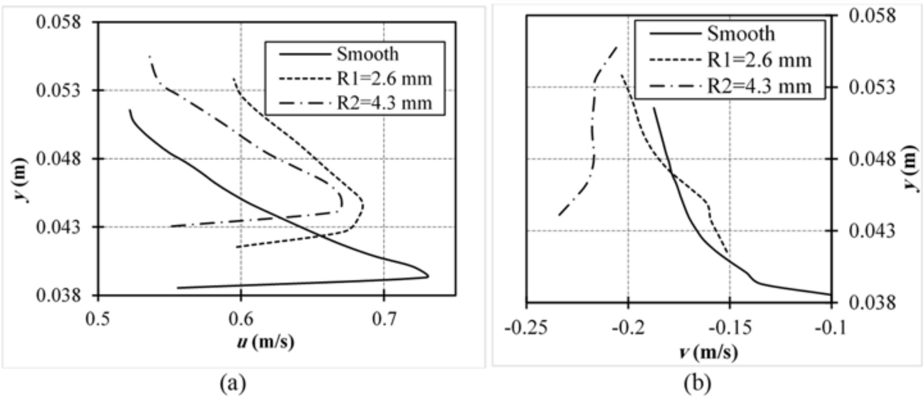

Figure (2): Velocities for QRC at $q = 8\times10^{-3}$ m²/s and $x = 0.075$ m: (a) u-velocity; (b) v-velocity

EXPERIMENTAL RESULTS AND DISCUSSION

Time-averaged Velocities

The smooth and roughened crest velocity data was compared by crest shape at the higher unit discharge ($q = 8\times10^{-3}$ m^2/s). Figure 2-a shows the QRC smooth-and rough-crest u-velocity profiles along a vertical traverse at $x = 0.075$m (downstream end of the crest profile). The maximum u-velocities for both the smooth- and the rough-crest cases occurred low in the water column (close to the crest boundary) and the minimum u-velocity occurred higher up near the free surface. Figure 2-a shows a reduction in the maximum u-velocity resulting from the added crest roughness; the roughened crest maximum u-velocity location shifted slightly higher in the water column for both roughness materials, relative to the smooth crest. A similar upward shift in the u-velocity was observed in the study of Felder and Islam (2016) on the rough embankment crest. The data also implies that the added roughness increases flow depth (reduced hydraulic efficiency) relative to the smooth crest (i.e., u-velocity data extends to larger y values for roughened crests). This is likely due to the added shear stress and resistance of flow passing over and through the porous roughness material. This finding shows a good agreement with the study of Felder and Islam (2016) who found that the rough-crest calculated shear stress for the embankment crest exceeded the smooth-crest case. The reduction in u-velocity modestly increases with increasing roughness of material height. Numerically, u-velocity decreased 6.2% and 8.2%, for $R_1 = 2.6$ mm and $R_2 = 4.3$ mm, respectively.

Figure 2-b shows the QRC v-velocity profiles across a vertical traverse for the smooth- and rough-crest cases at the same measurement station ($x = 0.075$ m, downstream end of the crest profile). For the smooth- and rough-crest cases, the maximum v-velocity occurred near the free water surface (free surface drawdown effects). In general, the v-velocity values increase in the downward direction (i.e., larger negative numbers) with the added crest roughness, which suggests that free surface drawdown effects amplify as a result of a deeper flow column created by the added flow resistance of the roughened crest boundary. The difference between maximum and minimum v-velocities reduced (i.e., v-velocity becomes more uniform with increasing crest roughness).

The influence of roughening the crest on the u- and v-velocities profiles for the QRC at a higher q (32×10^{-3}

m²/s) is shown in Figure 3. The crest roughness at the higher q has a similar trend to the lower q, but the influence of the roughness diminishes as shown by the modest changes in the u-velocity magnitudes. The decreasing percentages in the maximum u-velocity for R_1 = 2.6 mm and R_2 = 4.3 mm are 1.9% and 2.8%, respectively. The v-velocity profiles again indicate increasing flow depth with increasing roughness. The R_2 roughness produced a much higher magnitude (in the negative downward direction), relatively uniform v-velocity profile, compared to the smooth-crest profile. The R_1 roughness v-velocity fell between those two trends.

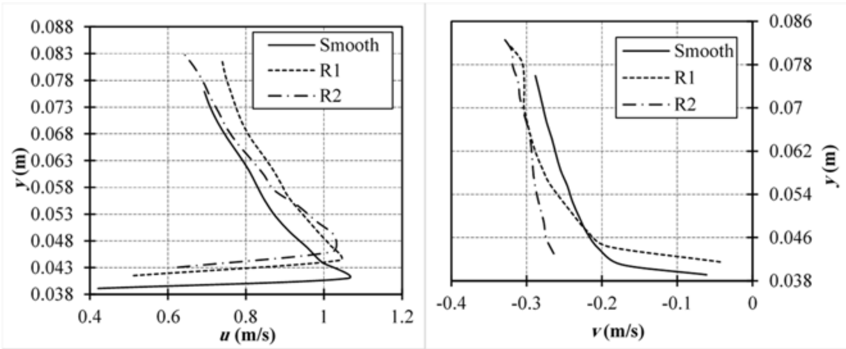

(a) (b)

Figure (3): Velocities for QRC at q = 32×10⁻³ m²/s and x = 0.075 m: (a) u-velocity; (b) v-velocity

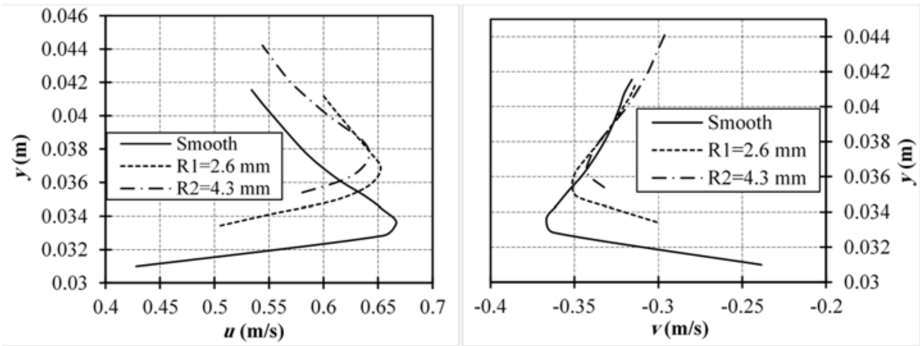

(a) (b)

Figure (4): Velocities for HRC at q = 8×10⁻³ m²/s and x = 0.05 m: (a) u-velocity; (b) v-velocity

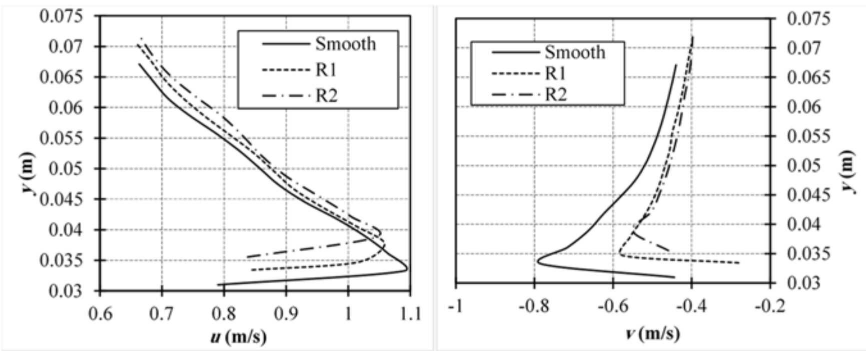

(a) (b)

Figure (5): Velocities for HRC at q = 32×10⁻³ m²/s and x = 0.05 m: (a) u-velocity; (b) v-velocity

The *u*- and *v*-velocities for the smooth and rough HRC cases ($q = 8\times10^{-3}$ m^2/s) along a vertical traverse at $x = 0.05$ m are represented in Figure 4. The *u*-velocity profile data [Figure 4-a] followed similar trends to the QRC data, with the maximum *u*-velocity also occurring lower in the water column for both the rough- and smooth-crest configurations and the maximum *u*-velocity values reducing with increasing roughness. Unlike the QRC, however, *v*-velocity decreased with roughness [Figure 4-b]. The reduction in the *u*-velocity is proportional to the roughness height, decreasing 2.2% and 3.8% for R_1 = 2.6 mm and R_2 = 4.3 mm, respectively. Unlike the QRC, the HRC *v*-velocity profiles, similar to the *u*-velocity profiles, increase initially (become more negative) until the maximum value has been reached and then decrease with increasing the distance from the crest. The *u*- and *v*-velocity maximum values occurred at relatively similar depths for common crest configurations. HRC flow depths also increased with increasing roughness.

The effect of crest roughening on the velocity profiles at the higher *q* (32×10^{-3} m^2/s) for the HRC is shown in Figure 5 at $x = 0.05$ m. Adding the roughness to the HRC with the higher *q* reduces the maximum *u*-velocity more, percentage wise, than at the lower *q*; *u*-velocity decreased by 2.9% and 4.1% for R_1 = 2.6 mm and R_2 = 4.3 mm, respectively (see Figure 5-a). Similar to the lower *q*, the HRC higher *q* maximum *v*-velocity decreased and the flow depth increased with increasing roughness [see Figure 5-b].

Figure 6 shows the smooth and rough (R_2 only) REC *u*- and *v*-velocity profile for $q = 8\times10^{-3}$ m^2/s at $x = 0.075$ m (downstream edge of the crest). As can be seen from Figure 6-a, the maximum *u*-velocity decreased around 1.6% when the roughness (R_2 = 4.3 mm) was added to the crest, the velocity profile shifted upward in the water column and the flow depth increased. The *v*-velocity increased and the profile became more uniform with roughness, similar to the QRC at the lower *q*. Figure 7 shows the smooth and rough REC *u*- and *v*-velocity profile across a vertical traverse for $q = 32\times10^{-3}$ m^2/s at $x = 0.075$ m (downstream edge of the crest). Figure 7-a shows that the rough-crest maximum *u*-velocity decreases (~1.1%) relative to the smooth crest. The velocity profile shifted upward in the water column and the flow depth increased. Figure 7-b shows that the *v*-velocity decreased slightly with roughness, confirming the increase in flow depth.

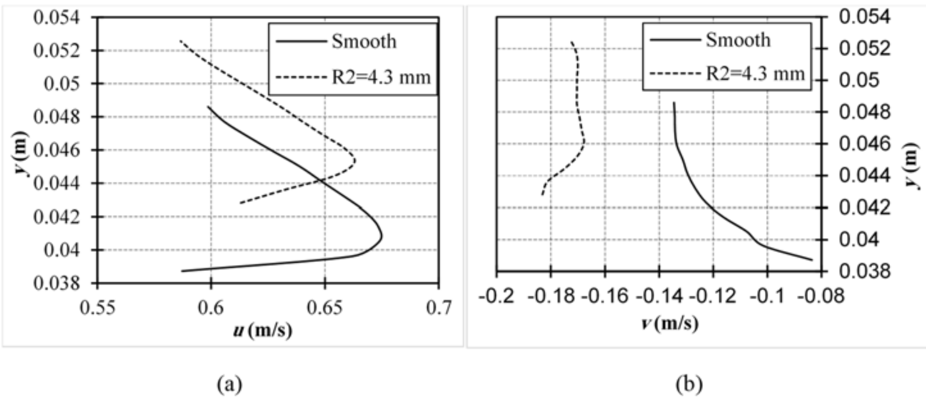

Figure (6): Velocities for REC at $q = 8\times10^{-3}$ m^2/s and $x = 0.075$ m: (a) *u*-velocity; (b) *v*-velocity

The data in Figures 2-7 shows a common behavior for the influence of adding roughness to the crest: reduced maximum *u*-velocity, shifting the velocity profile upward regardless of the discharge and crest shape and increasing flow depth. Though the reduction in the *u*-velocities is relatively small (1.1% to 8.2%), it is apparently significant enough to change the behavior of the boundary layer and add stability to the nappe. Changes to boundary-layer development caused by adding roughness could also be responsible for changes to nappe stability. The reduction in the maximum *u*-velocity is significant at the low discharge and/or large roughness and less significant at the higher discharge and/or smaller roughness. The roughness materials (R_1 and R_2) used in this study were sufficient to change the flow characteristics and produce a stable nappe. As mentioned previously, preliminary tests showed that a finer wire mesh roughness < 2 mm did not eliminate nappe instabilities in this small prototype-scale laboratory weir model. Note that the *u*- and *v*-velocity data in Figures 2-7 for the smooth and rough crests was evaluated at only one location (vertical traverse) per weir shape [x = 0.075 m (REC, QRC), x = 0.05 m (HRC)]. These locations represent the flow separation point from the crest profile for the REC, QRC and HRC profiles, which is likely significant, because these locations should correspond to the region of nappe-instability initiation. Though not presented herein, the u-velocity profiles showed similar magnitude-reduction behavior and increasing flow depth with increasing roughness over the full length of the crest.

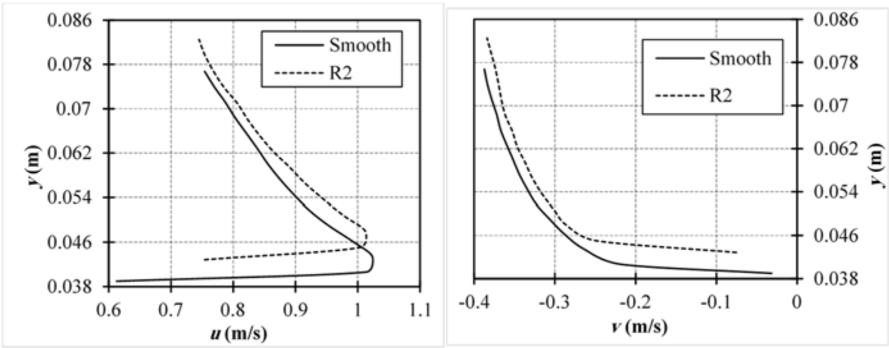

(a) (b)

Figure (7): Velocities for REC at q = 32×10^{-3} m^2/s and x = 0.075 m: (a) u-velocity; (b) v-velocity

Nappe Profile

Roughening the weir crest also influenced the nappe trajectory. Figure 8-a shows the nappe trajectories for the smooth and roughened QRC (q = 32×10^{-3} m^2/s). The nappe trajectories become steeper [reduced travel distance in the downstream (x) direction] with increased roughness, as would be expected with the corresponding reduction in the maximum u-velocity. For all three crest shapes and the specific discharges evaluated, the nappe became more stable with decreasing q. For roughened crests with a non-vented nappe, the shorter nappe trajectory means a smaller volume of trapped air behind the nappe, which may also positively impact nappe stability.

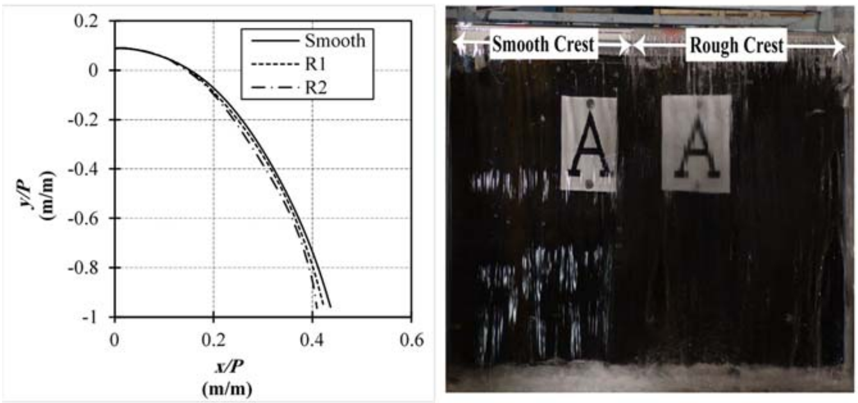

(a) (b)

Figure (8): (a) Nappe trajectory profile as a function of surface roughness, (b) Influence of crest

Discharge Coefficient (C_d)

C_d data summarized in Table 1 as a function of crest shape, discharge and roughness shows decreasing C_d with increasing roughness for all crest shapes tested. For all crest shapes, as q increases, the effect of the crest roughness on C_d decreases. These findings are consistent with those of Othman et al. (2011), Parilkova et al. (2012), Jalil et al. (2014) and Felder and Islam (2016) regarding C_d trends and weir crest roughness. If crest roughness is to be used as a remediation technique for nappe oscillation, C_d should be adjusted accordingly when evaluating the head-discharge curve *via* Eq. (1).

The diminishing change in C_d with increasing discharge suggests that adding roughness to a weir crest to mitigate nappe oscillation may have minimal effect on the upstream head required to pass the design flood, relative to the smooth crest.

Roughening the crest also resulted in the lower nappe surface (i.e., nappe surface closest to the weir wall) developing surface waves as shown in Figure 8-a. To illustrate this phenomenon, a half of the weir length was roughened and the other half left smooth; a letter "A" was attached to the downstream side of the weir wall in each section and photographed (see Figure 8-b). The "A" behind the nappe of the smooth crest is relatively undistorted; the "A" behind the rough crest nappe is significantly distorted. Some researchers (Kyotoh, 2002) suggest that the surface tension of water and air shear waves has a significant effect on the nappe stability. Roughening the crest may cause a reduction in the surface tension and the nature of the shear stress at the air-water interface such that the nappe becomes more stable.

Table 1. Summary of discharge coefficient (C_d) as a function of crest surface roughness, flow rate and crest shape

Crest Shape	Roughness	$q = 4\times10^{-3}$ m²/s		$q = 8\times10^{-3}$ m²/s		$q = 16\times10^{-3}$ m²/s		$q = 32\times10^{-3}$ m²/s	
		C_d	% Δ C_d	C_d	% Δ C_d	C_d	% Δ C_d	C_d	% Δ C_d
QRC	Smooth	0.789	0	0.698	0	0.686	0	0.693	0
	R_1	0.659	-16.5	0.638	-8.6	0.641	-6.6	0.668	-3.6
	R_2	0.607	-23.1	0.596	-14.6	0.623	-9.2	0.649	-6.3
HRC	Smooth	0.843	0	0.768	0	0.774	0	0.795	0
	R_1	0.719	-14.7	0.711	-7.4	0.719	-7.1	0.752	-5.4
	R_2	0.641	-23.9	0.649	-15.5	0.694	-10.3	0.713	-10.3
REC	Smooth	0.547	0	0.541	0	0.537	0	0.568	0
	R_1	0.475	-13.2	0.507	-6.2	0.518	-3.6	0.561	-1.3
	R_2	0.434	-20.7	0.479	-11.5	0.502	-6.5	0.547	-3.7

CONCLUSIONS

The influence of roughening the crest surface on the nappe stability was experimentally investigated using non-intrusive Particle Image Velocimetry (PIV) techniques. Velocity field measurements, discharge coefficient and nappe trajectory profiles were evaluated for smooth and different-roughness heights and different crest shapes including rectangular, quarter-rounded and half-rounded crests. On the basis of the results of this study, the following conclusions can be drawn:

1. The maximum horizontal velocity was found to be near the crest wall instead of near the free surface.
2. Adding the roughness to the crest causes the maximum horizontal velocity to decrease and shift higher up in the water column.
3. Over the range of q that resulted in nappe oscillations, the percent reduction in the maximum horizontal velocity caused by crest roughness was more significant for lower q values than for higher q values.
4. For the model scale tested, an approximate material roughness thickness ($R < 2$ mm) did not improve nappe stability. This limit is very specific to the particular roughness material used in the study (i.e., expanded metal mesh). Roughening materials with $R > 2$ mm were effective in stabilizing the nappe.
5. If reducing the maximum horizontal velocity through adding crest roughness is a key factor in eliminating nappe oscillations, the results of this study showed that even small reductions in the maximum horizontal velocity (~1.1%) corresponded to a nappe transitioning from being unstable to being stable.
6. Adding the roughness to the crest surface reduces the nappe profile trajectory (i.e., the nappe profile moves closer to the downstream weir wall), which in turn reduces the volume of the trapped air behind the nappe.
7. Most notably at lower q values, adding crest

roughness has a negative impact on the weir discharge efficiency as illustrated by the increased upstream flow depth and decreasing discharge coefficient values, relative to the smooth crest.

8. Adding crest roughness results in the formation of nappe surface waves (upstream face closest to the downstream weir wall), which may suggest that the nature of the surface tension and shear stress at that air-water interface may be altered due to the crest roughness.

Data-availability Statement

Some or all data, models or codes that support the findings of this study are available from the corresponding author upon reasonable request (velocities, pressure, water-surface elevation measurements).

Acknowledgments

Funding for this study was provided by the State of Utah and the Utah Water Research Laboratory.

REFERENCES

Anderson, A.A. (2014). "Causes and countermeasures for nappe oscillation". Master Thesis, Utah State University, Logan, UT.

Barlow, N.S., Helenbrook, B.T., and Lin, S.P. (2010). "Transience to instability in a liquid sheet". Journal of Fluid Mechanics, 666, 358-390.

Chanson, H. (2002). "The hydraulics of stepped chutes and spillways". 1st Edn., Swets & Zeitlinger B.V., Lisse, Netherlands.

Felder, S., and Islam, N. (2016). "Hydraulic performance of an embankment weir with rough crest". Journal of Hydraulics Engineering, 143 (3). https://doi.org/10.1061/(ASCE)HY.1943-7900.0001255.

Ghobadian, R., Fattahi Chaghabagi, A., and Ahmadi, A. (2013). "Effect of crest roughness on flow characteristics over circular weirs". Civil Engineering Infrastructures Journal, 46 (2), 199-207.

Hayder, A.M. (2017). "A laboratory study on stilling basin with semicircular rough bed elements". Jordan Journal of Civil Engineering, 11 (2), 198-205.

Jalil, S.A., Ibrahim, S.S., and Jafer, R.A. (2014). "Surface roughness effects on discharge coefficient of broad crested weir". Research Journal of Applied Sciences, Engineering and Technology, 7 (24), 5227-5233.

Khodier, M.A., and Tullis, B.P. (2017). "PIV measurements for oscillating liquid nappe". Journal of Hydro-environmental Research. https://doi.org/10.1016/j.jher.2017.11.002/

Kyotoh, H. (2002). "Incipient oscillations of a sheet of falling water and the instability mechanisms". J. Hydroscience and Hydr. Engrg., 20 (1), 77-93.

Lodomez, M., Crookston, B.M., Tullis, B.P., and Erpicum, S. (2019). "Mitigation techniques for nappe oscillations on free-overfall structures". Journal of Hydraulics Engineering, 145 (2), 04018086. https://doi.org/10.1061/(ASCE)HY.1943-7900.0001558

Othman, K.I., Chilmeran, T.A., and Al-Hafith, I.A.I. (2011). "Effect of size and surface roughness of cylindrical weirs on overflow characteristics". Al-Rafidain Eng. J., 19(2).

Parilkova, J., Riha, J., and Zachoval, Z. (2012). "The influence of roughness on the discharge coefficient of a broad-crested weir". Journal Hydrol. Hydro-mech., 60 (2), 101-114.

Petrikat, I.K. (1958). "Vibration tests on weirs and bottom gates". Water Power, 10, 52-57.

Qian, St., Zhang, Y., Xu, H., Wang, Xs., Feng, Jg., and Li, Zx. (2021). "Effects of surface roughness on overflow discharge of embankment weirs". J. Hydro-dyn., 33, 773-781. https://doi.org/10.1007/s42241-021-0068-y.

Schwartz, H.I. (1966). "Edgetones and nappe oscillation". The Journal of the Acoustical Society of America, 39 (3), 579-582.

Simmons, W.P. (1964). "Experiences of the bureau of reclamation with flow-induced vibrations". Laboratory Report No. Hyd-538, Office of Chief Engineer, Division of Research, Hydraulics Branch, Denver, Colorado.

Squire, H.B. (1953). "Investigation of the instability of a moving-liquid film". British Journal of Applied Physics, 4, 167-169.

Taylor, G. I. (1959). "The dynamics of thin sheets of fluid-Part II. Waves on fluid sheets". Proceedings of the Royal Society of London, Series A, 253(1247), 296–312.

Water, M., Sewerage, and Board, D. (1980). "Investigation into spillway discharge noise at Avon dam". ANCOLD Bulletin, (57), 31-36.